



Investigation of the structure in oxyfluoride $\text{TeO}_2\text{--P}_2\text{O}_5$ based glasses with the various BaF_2 content

M. Lesniak^{a,*}, G. Mach^a, B. Starzyk^a, A. Baranowska^b, M. Bik^a, M. Kochanowicz^b, J. Zmojda^b, P. Miluski^b, M. Sitarz^a, D. Dorosz^a

^a AGH University of Science and Technology, Faculty of Materials Science and Ceramics, A. Mickiewicza 30 Avenue, 30-059, Krakow, Poland

^b Bialystok University of Technology, Faculty of Electrical Engineering, Wiejska Street 45D, 15-351, Bialystok, Poland

ARTICLE INFO

Article history:

Received 21 February 2020

Received in revised form

12 May 2020

Accepted 13 May 2020

Available online 16 May 2020

Keywords:

Oxyfluoride phosphate-tellurite system

BaF_2

Glass structure

³¹P MAS NMR

ABSTRACT

A series of samples containing the phosphate and tellurite glass formers were prepared by varying the barium fluoride concentration from 0 to 30 mol %. The results of the XRD analysis indicated that barium fluoride in the 5–30 mol% content improved the glass-forming nature of oxyfluoride phospho-tellurite glasses in the $\text{TeO}_2\text{--P}_2\text{O}_5\text{--BaF}_2\text{--ZnF}_2\text{--Na}_2\text{O--ErF}_3$ system. For 0 mol% of BaF_2 amount, the glass-ceramic sample was obtained with ErPO_4 (erbium phosphate V) crystallines in the glassy host. The structure of the obtained glasses were investigated by using Mid-infrared, Raman, and ³¹P MAS NMR spectroscopy. Herein in this work, the results suggested that the addition of BaF_2 depolymerized network of glasses, effected in the conversion of $\text{Te}(\text{O,F})_4$ into $\text{Te}(\text{O,F})_3$, $\text{Te}(\text{O,F})_{3+1}$ units, as well as P^2 into P^1 and P^0 units.

© 2020 Elsevier B.V. All rights reserved.

1. Introduction

Recent advances in the application of optic and photonic devices and components from visible (VIS) to infrared (IR) region contributed to the increase in interest of the study of optically transparent glass and glass-ceramic materials doped with rare-earth ions (RE). Among various kinds of oxide glass hosts available in the literature (silicate, phosphate, borate, germanate), tellurite glasses appear to be a very interesting and attractive glass matrix for rare-earth ions [1–7]. Tellurite glasses are characterized by low phonon energy ($\sim 750\text{ cm}^{-1}$), low melting temperature (around $400\text{ }^\circ\text{C}$), high refractive index, large transparency window ($0.4\text{--}5\text{ }\mu\text{m}$), and high thermal and chemical stability [5–9]. These interesting physical properties of tellurite glasses enable them for the following applications: glass fibers for near- and mid-infrared nonlinear applications [10,11], laser writing [12], optical sensor [13,14], solar cell [15,16] and biomedical applications [17]. However, without other types of glass formers (e.g. B_2O_3 , GeO_2 , P_2O_5), and modifiers (alkali or/and alkaline earth oxides), tellurium oxide does not have the ability to compose a vitrified states in the melt quenching procedure [5–17]. Moreover, adding to the second glass network

former to the tellurite glass matrix is an interesting subject of study due to the unique properties of mixed network glasses [18,19]. Phosphate glasses have been of research interest in the field of materials for optical applications for many years. Due to their unique physicochemical and spectroscopic properties, they have been used for the production of lasers [20], optical fibers [21], optical amplifiers [22] and sensors [23]. In addition, phosphate glasses are characterized by, among others, high transmittance and low refractive index. Glasses based on P_2O_5 doped with Er^{3+} , Pr^{3+} , Yb^{3+} , Nd^{3+} , and Tm^{3+} ions emit near-infrared radiation and are used in telecommunications windows [24–26]. Glass co-doped with Eu^{3+} , Dy^{3+} , Tb^{3+} , and Sm^{3+} ions are known as light-emitting materials in the visible range [24,27,28]. In that sense, the combination of TeO_2 and P_2O_5 glass formers appears to be a very interesting issue in the case of designing and obtaining mix network glasses [29–32]. The addition of the P_2O_5 leads to an improvement in some interesting properties of the tellurite host such as glass transition temperature, thermal expansion coefficient (TEC), refractive index, transmissivity in the ultraviolet and infrared regions, chemical durability and third-order non-linear susceptibility [33–35].

Based on previous studies, it was found that oxide glasses and glass-ceramic based on $\text{TeO}_2\text{--P}_2\text{O}_5$ system doped with different rare-earth oxides are characterized by the interesting thermal and optical properties [36–46]. Abdel-Kader et al. studied the thermoluminescence dosimetry of the La_2O_3 , CeO_2 , Sm_2O_3 and Yb_2O_3

* Corresponding author.

E-mail address: mlesniak@agh.edu.pl (M. Lesniak).

doped phospho-tellurite glasses [36]. Nandi et al. investigated the physical, thermal and spectroscopic properties of erbium-doped phospho-tellurite glasses in comparison with a tellurite glass without P_2O_5 [37]. In this paper was shown, that the transparency of the glass towards UV was enhanced by the addition of phosphate and the Ω_2 , Ω_4 intensity parameters of phospho-tellurite glasses were low comparing to the glass without phosphate [37]. Recently, the data about fabrication and spectroscopic properties of the Yb-doped and Yb–Er-codoped tellurite-phosphate glass fibers suitable for superfluorescence fiber sources (SFS) have been published [38]. Spectroscopic properties of phospho-tellurite glasses were investigated in the Er^{3+} -doped $NaPO_3$ – TeO_2 – ZnO – Na_2O system [39]. Influence of europium ions on structural behavior in the phospho-tellurite glasses within a concentration range, 0–30 mol% of the Eu_2O_3 , has been investigated using infrared spectroscopy [40]. Based on the obtained IR spectra of samples, it has been shown, that europium ions with amount up to 5 mol % into the chemical composition of the glasses were network former ions, however, presence of the Eu^{3+} in the 10–30 mol % range in glasses caused the decrease in the connectivity of glass network [40]. The increase in the concentration of europium ions, over 40 mol%, resulted in the transformation of trigonal bipyramids into trigonal pyramids units and the disappearance of the P=O stretching bond in $[PO_4]$ tetrahedron. This has led to a decrease in the connectivity of the glass network and the formation of the $EuPO_4$ crystalline phase (glass-ceramic sample) [40]. Optical absorption and photoluminescence properties of Yb^{3+} – Ho^{3+} co-doped phospho-tellurite glasses have been also investigated [41]. The detailed study on the effects of P_2O_5 contents on the spectroscopic properties of Er^{3+} -doped TeO_2 – ZnO – Na_2O glasses as potential optical glasses for fiber amplifiers was performed by Jlassi et al. [42]. In this paper [42], the addition of the P_2O_5 enhanced the local symmetry around erbium ions and PL life time became longer. The solid phospho-tellurite photonic bandgap fiber with two layers of high-index rods (TeO_2 – Li_2O – WO_3 – MoO_3 – Nb_2O_5 , TLWMN) in the cladding (TeO_2 – ZnO – Li_2O – K_2O – Al_2O_3 – P_2O_5 , TZLKAP) were reported by Cheng et al. [43]. Neodymium-doped tellurite glasses with varying P_2O_5 concentrations in the TeO_2 – P_2O_5 – Al_2O_3 – K_2O – La_2O_3 – Nd_2O_3 system were investigated and spectroscopy was characterized by Linganna et al. [44]. Jlassi et al. [45] shown that by adding P_2O_5 to tellurite glasses in the TeO_2 – ZnO – Na_2O – Er_2O_3 system, thermal stability, spectroscopic quality factor, and high gain of these glasses were improved. Luminescence improvement of Er^{3+} ions in phospho-tellurite glass-ceramic in the TeO_2 – ZnO – Na_2O – P_2O_5 – Er_2O_3 system, containing nanocrystals of α - TeO_2 , β - TeO_2 , and $ErPO_4$, phases was achieved by Ennouri et al. [46].

The papers [36–46] confirm that the second former oxide like P_2O_5 improves both the thermal and the optical properties of RE doped oxide tellurite glasses. However, these papers mainly relate to the structure and properties (thermal, spectroscopic) of the simple co-doped TeO_2 – P_2O_5 – ZnO – Na_2O oxide system. Literature reports show that oxyfluoride phosphate-tellurite glasses are less frequently used in optical technology [47,48]. However, the oxide phosphate-tellurite glass has absorbed hydroxyl groups in the glass host and phosphate-tellurite glass fiber with low-loss is not easy to be prepared due to the inhomogeneity of this glass [49]. The high concentration of OH^- ions in the glass matrix results in the quenching of luminescence of lanthanide ions in the glassy host. The addition of fluorides it is an effective way to exhaust OH^- content due to the reaction of $OH^- + F^- \rightarrow O^{2-} + HF\uparrow$. Additionally, the oxyfluoride glasses have been widely investigated as glassy host materials for RE ions because they have better mechanical and chemical stabilities than fluoride glasses and present low phonon energy compared to oxide glasses [50].

The recent developments in the oxyfluorotellurite glasses doped

with different lanthanides are also reported about the zinc-tellurite glass system. Spectroscopic studies of the Tm^{3+}/Yb^{3+} co-doped TeO_2 – ZnF_2 – PbO – Nb_2O_5 [51], Ho^{3+}/Yb^{3+} co-doped TeO_2 – ZnF_2 [52] and Er^{3+}/Yb^{3+} co-doped TeO_2 – PbF_2 – ZnF_2 [53] oxyfluorotellurite glasses were successfully prepared by using melt quenching method. In the literature can be found only a few studies about the simple oxyfluoride phospho-tellurite glass system [47,48].

In previous work [48], we studied the effect of erbium fluoride addition on thermal, structural, and spectroscopic properties of oxyfluoride phosphate-tellurite precursor glass in the multicomponent TeO_2 – P_2O_5 – BaF_2 – ZnF_2 – Na_2O – ErF_3 system for transparent active glass-ceramic. Based on the knowledge that the development of phospho-tellurite glasses in the multicomponent system requires expertise of their structural chemistry, which is also fundamental to design these glasses for practical application, in the present paper we studied vitreous domain of the TeO_2 – P_2O_5 – BaF_2 – ZnF_2 – Na_2O – ErF_3 system in the relation of BaF_2 concentration. One objective of the study was to determine the impact of the systematically changing BaF_2 content on the network structure of erbium-doped oxyfluoride phosphate-tellurite glasses using XRD, MIR, Raman, and ^{31}P MAS NMR methods.

2. Experimental

The oxyfluoride phosphate-tellurite samples of the following composition $(69.5-x) TeO_2$ – $10P_2O_5$ – $xBaF_2$ – $20(ZnF_2$ – $Na_2O)$ – $0.5ErF_3$ $x = 0, 5, 10, 15, 20, 25, 30$ mol % were prepared as described in the paper [48]. The samples were noted according to the barium fluoride content into chemical composition: TP0BaF₂, TP5BaF₂, TP10BaF₂, TP15BaF₂, TP20BaF₂, TP25BaF₂ and TP30BaF₂.

The nature of the samples was confirmed through X-ray studies with X'Pert Pro X-ray diffractometer supplied by PANalytical with Cu $K_{\alpha 1}$ radiation ($\lambda = 1.54056 \text{ \AA}$) in the 2θ range of 10–80°. Qualitative identification of the phase composition was performed with reference to the ICDD PDF-2 database.

The microstructure of the glass-ceramic sample was investigated by NOVA NANO SEM 200 scanning electron microscope with the EDS microanalyzer. Observations and analyses were performed in a low vacuum by using a detector LVD and at an accelerating voltage in the range of $10e^{18}$ kV.

The MIR spectra of the glasses were obtained with the Fourier spectrometer (Bruker Optics-Vertex70 V). The measurements were done using the KBr pellet technique. Absorption spectra were recorded at 128 scans and the resolution of 4 cm^{-1} .

Raman spectra of all glass samples were obtained using a Lab-RAM HR spectrometer (HORIBA Jobin Yvon, Palaiseau, France) using the excitation wavelength of 532 nm. The diffraction grating was 1800 lines/mm. The spectra were recorded in several points with the standard spot of about 1 μm . The standard deviation of the position and full width at half maximum (FWHM) of each of the component MIR and Raman bands was $\pm 4 \text{ cm}^{-1}$.

The ^{31}P MAS NMR spectra of glasses were recorded using spectrometer probe Apollo-type by Tecmag.

MIR, Raman and ^{31}P MAS NMR spectra of glasses have been normalized and then deconvoluted using Fityk software (0.90.8 software). The coefficient of determination (R squared) of all the deconvoluted spectra was 0.99.

3. Results and discussion

All of the prepared samples containing BaF_2 (TP5BaF₂–TP30BaF₂) were homogeneous and transparent. The amorphous nature of these samples (glasses) was confirmed by the absence of any peaks

and intense broad humps in the 20–35° range of the two theta angles in the diffractograms patterns (Fig. 1). The sample without BaF₂ (TPOBaF₂) was opaque. Based on the XRD (Fig. 2a) and SEM-EDS (Fig. 2b) studies, it was found that obtained material is glass-ceramic with ErPO₄ (erbium phosphate V) crystallines (JCPDF 01-083-0662) incorporated in the glassy host. As can be seen from Figs. 1 and 2, the addition of BaF₂ improved the glass-forming nature of the oxyfluoride phosphate-tellurite system. According to the literature [47,54], the addition of alkaline earth oxides such as CaO improves the glass-forming nature of tellurite glasses. The vitreous state in the TeO₂–P₂O₅–BaF₂–ZnF₂–Na₂O–ErF₃ system in the function of the BaF₂ content was shown in Fig. 3.

The structural changes in tellurite glass networks have been the subject of numerous studies [55–58]. In the alkali-tellurite oxide glass, it was found that its structure is created by [TeO₄] four coordinated trigonal bipyramids (Te⁴₄ and Te³₄) and [TeO₃] three coordinated trigonal pyramid (Te²₃, Te¹₃, and Te⁰₃), where n represents the number of bridging oxygens and m is the coordination number in Teⁿ_m units [59–61]. These five tellurium polyhedra have been identified from crystalline TeO₂, and all have been suggested to be present to some extent within tellurium glass systems [62,63].

The basic building units of crystalline and amorphous phosphates are the P-tetrahedra. These tetrahedra link through covalent bridging oxygens to form various phosphate anions and are classified using the Pⁱ terminology, where i represents the number of bridging oxygens/fluorides. Phosphate glasses can be made from a cross-linked network of P³ tetrahedra, metaphosphate chains of P² tetrahedra and pyro- (P¹) and orthophosphate (P⁰) units. The addition of modifying cations to the network of the tellurite and phosphate glasses results in the creation of non-bridging oxygens/fluorides at the expense of bridging oxygens/fluorides (depolymerization of the network) [64–66].

In this paper, the terminology described above has been used to the characterization of network of the oxyfluoride phosphate-tellurite glasses in the TeO₂–P₂O₅–BaF₂–ZnF₂–Na₂O–ErF₃ system.

The normalized MIR spectra in the 1300–520 cm⁻¹ range of all glasses with varying BaF₂ concentrations have been showed in Fig. 4a. All MIR spectra present major bands that are characteristic for tellurite glasses and typical structural units in the phosphate glasses [48,54]. As can be seen from Fig. 4a, the intensities of the individual bands on the MIR spectra were changed with the varying BaF₂ content in the chemical composition of glasses. In order to

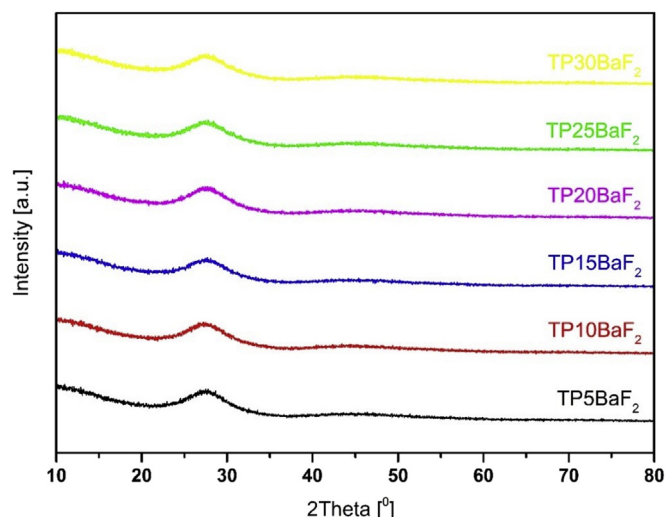


Fig. 1. Diffraction patterns of the sample with 5–30 mol% BaF₂ content.

determine the changes in the intensities of bands on the MIR spectra of the glasses, the deconvolution has been performed for the MIR spectra of the following glasses: TP5BaF₂, TP15BaF₂, and TP30BaF₂ (Fig. 4b–d). The parameters of the component bands have been shown in Table 1. The assignments of the individual bands, presented in Table 2, have been performed based on data available on oxide, fluoride and oxyfluoride tellurite, phosphate and phospho-tellurite materials [48,67–75].

On the all deconvoluted MIR spectra (Figs. 4b–d) thirteen component bands in the 1300–520 cm⁻¹ range can be seen. Bands at around 540 cm⁻¹ and 570 cm⁻¹ correspond to the asymmetric and symmetric bending deformation vibration of O,F–P–O,F bonds in P² units, respectively [48,67]. The bands at ~610 cm⁻¹ and ~670–680 cm⁻¹ can be assigned to the stretching vibrations of Te–O,F bonds in trigonal bipyramidal units Te(O,F)₄ (tbp) [48,68,69]. The presence of the band in the 660–690 cm⁻¹ range in the spectra of all glasses can be ascribed to the symmetric stretching vibration of F–P–F bonds [48,70]. The band at around 710–740 cm⁻¹ corresponds to the stretching vibrations of trigonal pyramidal units Te(O,F)₃ (tp) or Te(O,F)₃₊₁ polyhedra [69]. The next band in the deconvoluted spectra of the TP5BaF₂, TP15BaF₂ and TP30BaF₂ glasses (Figs. 4b–d), i.e. at around 760–780 cm⁻¹ can be assigned to the vibration of the continuous network composed of Te(O,F)₄ and Te–O,F stretching vibration of Te(O,F)₃₊₁ polyhedra and/or symmetric P–O, F=P bonds in P¹ units [48]. The band at ~790–800 cm⁻¹ is ascribed to the asymmetric stretching vibrations of Te(O,F)₃ (tp) units or Te(O,F)₃₊₁ polyhedra [48,71].

As can be seen in Figs. 4b–d and Table 1, the increase in BaF₂ addition into the chemical composition of glasses resulted in a shift of the band's position in the deconvoluted MIR spectrum of the TP5BaF₂ (Fig. 4b) glass at around 670 cm⁻¹, 718 cm⁻¹, and 766 cm⁻¹, 1092 cm⁻¹, 1154 cm⁻¹ to the higher wavenumbers, i.e. 675 cm⁻¹, 732 cm⁻¹, 771 cm⁻¹, 1110 cm⁻¹, 1170 cm⁻¹ (TP15BaF₂, Fig. 4c) and 687 cm⁻¹, 736 cm⁻¹, 770 cm⁻¹, 1102 cm⁻¹, 1164 cm⁻¹ (TP30BaF₂ glass, Fig. 4d). This fact can be explained by the replacement of fluoride with oxide ions leading to an increase in the strength of the bond (P–F, Te–F) compared to P–O and Te–O bonds [48].

According to the literature on the MIR spectra of P₂(O,F)₅ glasses, the band at around 870–880 cm⁻¹ can be attributed to the asymmetric stretching vibrations of P² units in the P₂(O,F)₅ glass [67]. The band at ~920 cm⁻¹ is ascribed to the stretching vibrations of P–O–P linked with metaphosphate chain and P–F groups in P² units [72,73]. The bands at around 970 cm⁻¹ and 1030 cm⁻¹ are due to the asymmetric stretching vibration of P–(O,F)⁻ bonds in P⁰ units [67] and the symmetric stretching vibrations of P(O,F)₃ groups in P¹ units, respectively [72]. The bands above 1050 cm⁻¹, i.e. at around 1100 cm⁻¹ and 1150–1170 cm⁻¹ are corresponded to the asymmetric stretching vibrations of P(O,F)²⁻ groups in P¹ units [48,74] and asymmetric stretching vibrations of non-bridging oxygen/fluoride in P² units [75], respectively.

The increase in fluorine ion content in all glasses due to the introduction of BaF₂ led to an increase in the integral intensity of the band at around 670–690 cm⁻¹, associated with symmetric stretching vibrations of the F–P–F bond from 72 (TP5BaF₂) up to 87 (TP15BaF₂) and to 98 (TP30BaF₂) - Figs. 4b–d, Table 1). It suggested, that fluoride ions substituted oxygen ions into the glass network.

Additionally, with increasing BaF₂ content, the integral intensities of the following bands have been increased (Figs. 4b–d, Table 1): at 543 cm⁻¹ from 7 (TP5BaF₂) to 14 (TP15BaF₂) and to 19 (TP30BaF₂) - band related to the asymmetric bending vibration of O–P–O bonds in P² units, at 978 cm⁻¹ from 43 (TP5BaF₂) to 51 (TP15BaF₂) and to 71 (TP30BaF₂) - band assigned to the asymmetric stretching vibration of P–(O,F)⁻ bonds in P⁰ units, and at 1090–1100 cm⁻¹ from 119 (TP5BaF₂) to 138 (TP15BaF₂) and to 162 (TP30BaF₂) - band corresponding to the asymmetric stretching

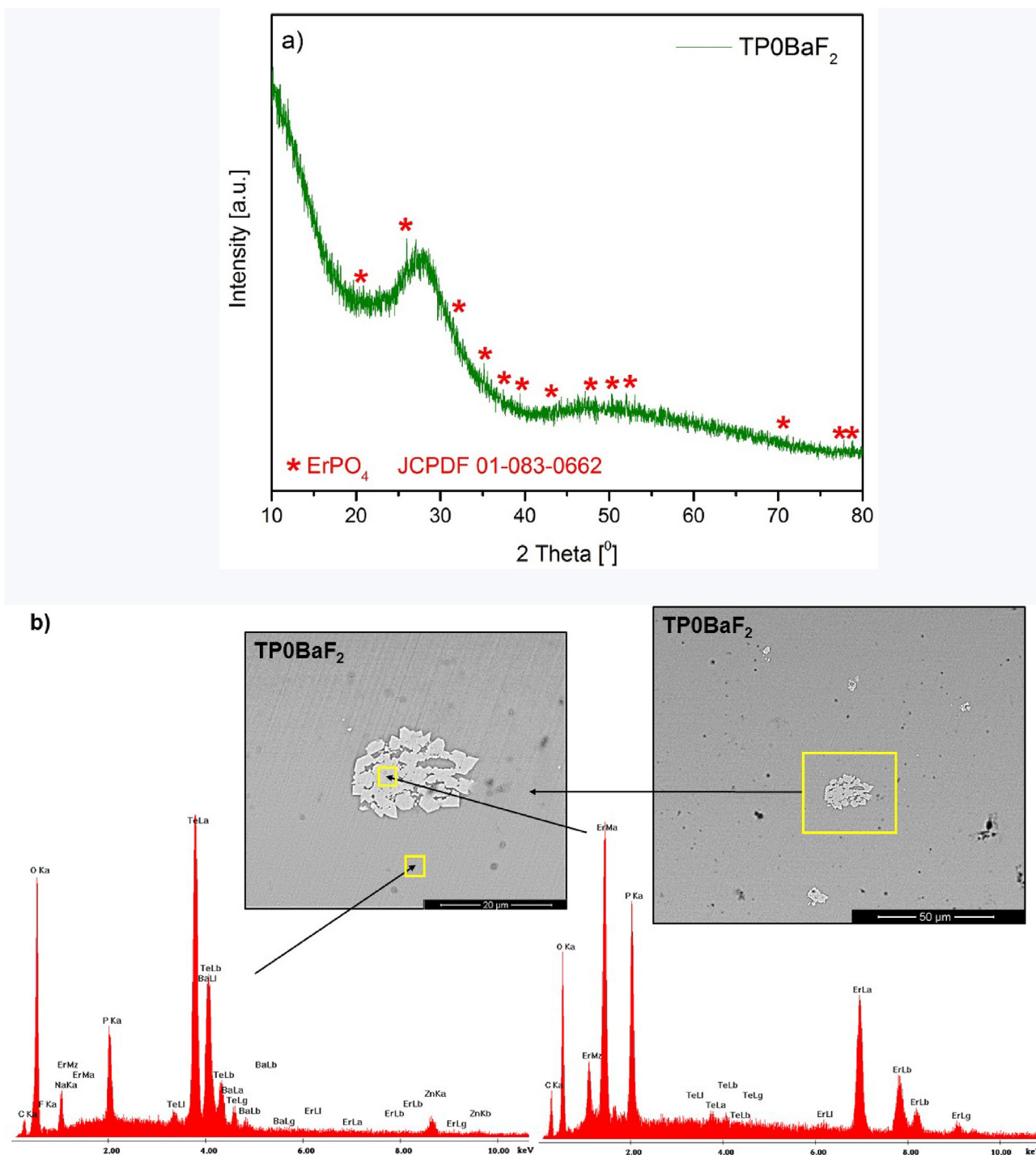


Fig. 2. Diffraction pattern a) and SEM-EDS photos b) of the TP0BaF₂ sample.

vibrations of P(O,F)²⁻₃ groups in P¹ units. The changes in the integral intensities of bands have resulted in the depolymerization of the glass phosphate subnetwork [76].

With the increase in the content of BaF₂, the decrease in the integral intensity of the band in the 760–770 cm⁻¹ range, i.e. from 61 (TP5BaF₂, Fig. 2, Table 1) to 27 (TP15BaF₂) and to 18 TP30BaF₂ glasses, Figs. 4b–d, Table 1) has been noted. The mentioned band is related to the vibration of the continuous network composed of Te(O,F)₄ and Te–O,F stretching vibration of Te(O,F)₃₊₁ polyhedra.

The decrease in intensity of this band is due to the reduced concentration of the TeO₂ oxide into the chemical composition of the glasses at the expense of introducing BaF₂.

Based on the deconvoluted MIR spectra (Figs. 4b–d) and spectral fitting parameters (Table 1), it can be concluded that the addition of BaF₂ resulted in an increase in the amount of the P¹ and P⁰ units at the expense of the amount of the P² units, according to the following equation: 2 P² ↔ P¹ + P⁰. With the addition of the BaF₂ the integral intensities of the bands related to the vibrations of

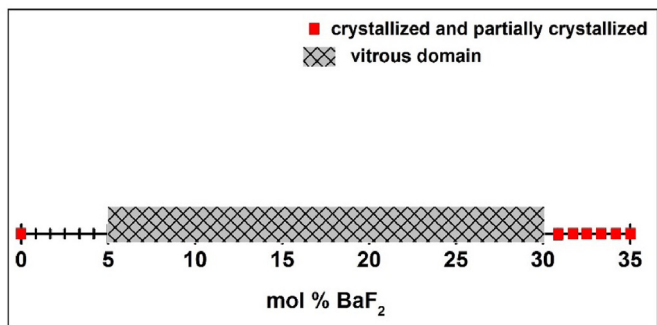


Fig. 3. Vitreous state in the $\text{TeO}_2\text{-P}_2\text{O}_5\text{-BaF}_2\text{-ZnF}_2\text{-Na}_2\text{O-ErF}_3$ system in the function of the BaF_2 content.

P^2 units decreased, i.e. bands at $\sim 920\text{ cm}^{-1}$ from 105 (TP5BaF₂) to 82 (TP15BaF₂) and to 56 (TP30BaF₂) and band in the 1150–1170 cm^{-1} range from 91 (TP5BaF₂) to 59 (TP15BaF₂) and to 50 (TP30BaF₂ glass) - Figs. 4b–d and Table 1.

As can be seen in Figs. 4b–d and Table 1, the integral intensity of the band at around 970 cm^{-1} related to the asymmetric stretching vibration of P-O^- bonds in P^0 units and band at around 1100 cm^{-1}

corresponding to the asymmetric stretching vibrations of P(O,F)^{2-3} groups in P^1 units increased with the raising content of BaF_2 from 43 (TP5BaF₂) to 51 (TP15BaF₂) and to 71 (TP30BaF₂), and from 119 (TP5BaF₂) to 138 (TP15BaF₂) and to 162 (TP30BaF₂), respectively.

Summarizing, the analysis of all MIR spectra of the glasses with varying BaF_2 content suggests that, the bridging bonds of the P-(O,F)-P , Te have been broken and the non-bridging bonds were formed as the number of barium ions increased in the chemical composition of the glasses. The phosphate chains have become shorter in the network of oxyfluoride phosphate-tellurite glasses [70–72].

Many authors suggested that OH absorption is a very serious problem in the development of the ultra-low loss oxyfluoride and fluoride fibers, as the OH stretching vibration occurs at around $3\text{ }\mu\text{m}$, closely from the minimum intrinsic absorption wavelength near $2.6\text{ }\mu\text{m}$. For this reason, great efforts have been made toward the preparation of high-quality glasses with minimum OH content [49,53].

To clarify the influence of BaF_2 concentration on the content of OH^- in the glasses, the MIR spectra of glasses in the $3600\text{-}3000\text{ cm}^{-1}$ range were presented in Fig. 5. It is well-known that band at around 3400 cm^{-1} corresponds to the free OH groups in glasses. It can be seen from Fig. 5 that the difference in the

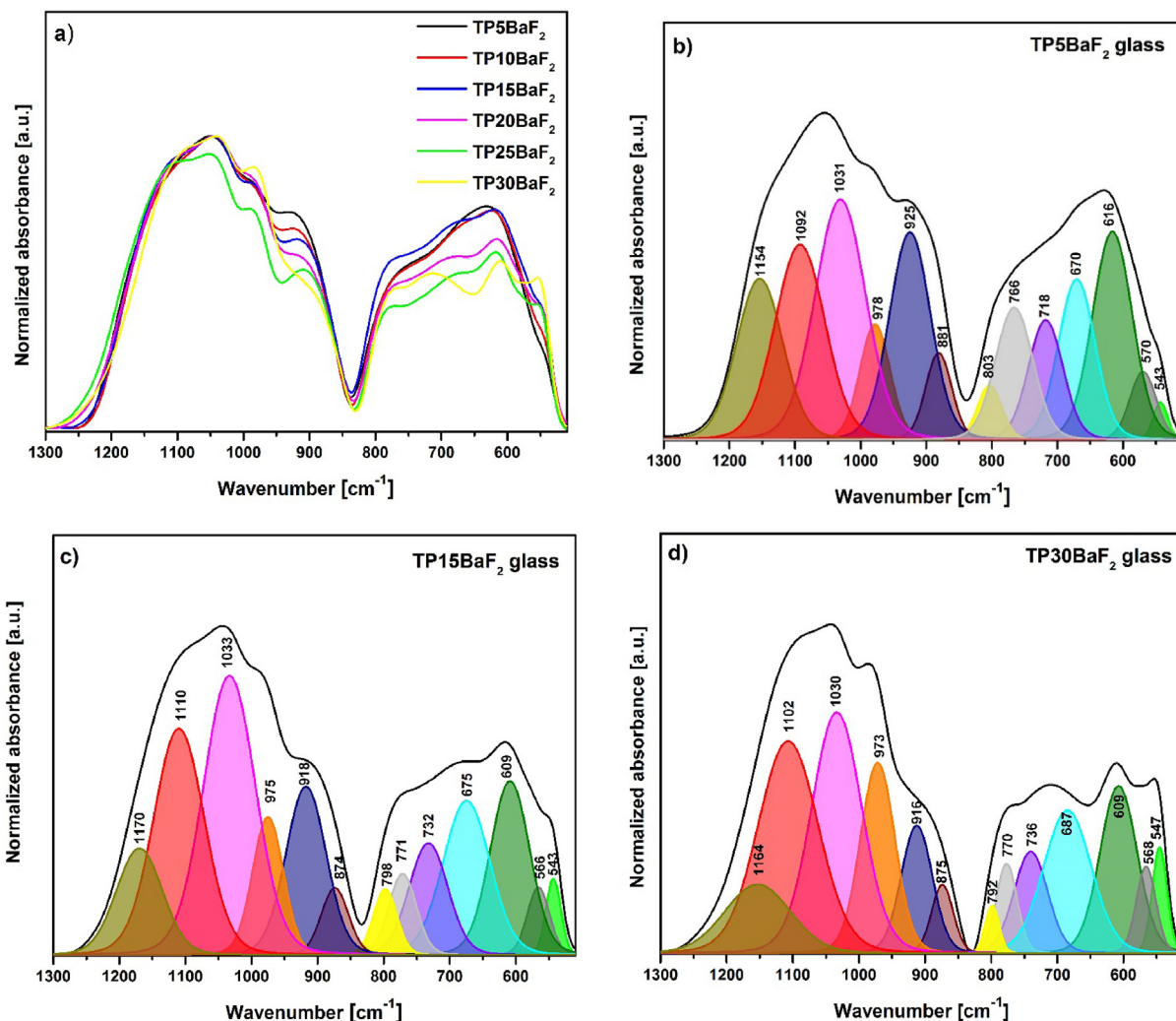
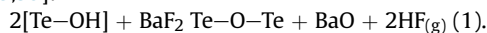


Fig. 4. MIR spectra in the $1300\text{-}520\text{ cm}^{-1}$ range of glasses with varying BaF_2 content a) and deconvoluted MIR spectra of TP5BaF₂ b), TP15BaF₂ c) and TP30BaF₂ d) glasses.

Table 1
MIR spectroscopy spectral fitting parameters spectra of TP5BaF₂, TP15BaF₂, and TP30BaF₂ glasses.

TP5BaF ₂ glass		
Peak [cm ⁻¹] (±4.0)	Integral intensity (±0.5)	FWHM [cm ⁻¹] (±4.0)
543	7	26
570	22	47
616	101	71
670	72	66
718	51	62
766	61	68
803	16	44
881	28	47
925	105	74
978	43	54
1031	149	91
1092	119	90
1154	91	83
TP15BaF ₂ glass		
Peak [cm ⁻¹] (± 4.0)	Integral intensity (± 0.5)	FWHM [cm ⁻¹] (± 4.0)
543	14	27
566	18	40
609	83	71
675	87	84
732	52	69
771	27	50
798	19	42
874	22	49
918	82	72
975	51	55
1033	176	93
1110	138	90
1170	59	82
TP30BaF ₂ glass		
Peak [cm ⁻¹] (± 4.0)	Integral intensity (± 0.5)	FWHM [cm ⁻¹] (± 4.0)
547	19	26
568	19	35
609	80	70
687	98	84
736	33	54
770	18	38
792	15	31
875	18	40
916	56	61
973	71	55
1030	138	82
1102	162	98
1164	50	100

absorption spectra of glasses can be related to the OH free groups, i.e. increase in BaF₂ content in the chemical composition of analyzed glasses was efficient in removing OH free groups. The addition of the BaF₂ led to a decrease in the intensity of the band at around 3430 cm⁻¹. The reduction of the OH free groups in glasses with the addition of BaF₂ can be related to the following reaction [49,53]:



Subsequently, HF was removed from the system and OH groups in the glasses were reduced with the addition of BaF₂.

In Fig. 6a, normalized Raman spectra of oxyfluoride phosphotellurite glasses with various concentrations of the BaF₂ have been shown. As can be seen in Fig. 6a, all Raman spectra were dominated by six bands at around 460 cm⁻¹, 560 cm⁻¹, 660 cm⁻¹, 790 cm⁻¹, 890 cm⁻¹ and 970 cm⁻¹. Above 20 mol % of BaF₂, an additional band appeared at around 350 cm⁻¹.

In order to assign all the component bands in Raman spectra to

Table 2
Band assignment.

Band position [cm ⁻¹]	Assignment
543/543/547	deformation vibration of asymmetric and symmetric bending O, F–P–O, F bonds in P ² units [48,67]
570/566/568	stretching vibrations of Te–O, F bonds in Te(O, F) ₄ (tbp) units [48,68]
616/609/609	stretching vibrations of Te–O, F bonds in Te(O, F) ₄ (tbp) units [48,69]
670/675/687	symmetric stretching vibration of the P–F bonds [70]
718/732/736	stretching vibrations of Te(O, F) ₃ (tp) units or Te(O, F) ₃₊₁ polyhedra [69]
766/771/770	the vibration of the continuous network composed of Te(O, F) ₄ and Te–O, F stretching vibration of Te(O, F) ₃₊₁ polyhedra or symmetric P–O, F–P bonds in P ¹ units [48]
803/798/792	asymmetric stretching vibrations of Te(O, F) ₃ (tp) units or Te(O, F) ₃₊₁ polyhedral [48,71]
881/874/875	asymmetric stretching vibrations of P ² units [67]
925/918/916	asymmetric stretching vibrations of P–O, F–P linked with metaphosphate chain and P–F groups in P ² units [72,73]
978/975/973	asymmetric stretching vibrations of P–(O, F) bonds in P ⁰ units [67]
1031/1033/1030	symmetric stretching vibrations of P(O, F) ²⁻³ groups in P ¹ units [72]
1092/1110/1102	asymmetric stretching vibrations of P(O, F) ²⁻³ groups in P ¹ units [48,74]
1154/1170/1164	asymmetric stretching vibrations of non-bridging oxygen/fluoride in P ² units [75]

appropriate vibrations, selected Raman spectra of the glasses have been deconvoluted. In Figs. 6b–d, the deconvoluted Raman spectra of TP5BaF₂ (Fig. 6b), TP15BaF₂ (Fig. 6c) and TP30BaF₂ (Fig. 6d) glasses have been presented. Parameters of the component bands on Raman spectra of the of TP5BaF₂, TP15BaF₂, and TP30BaF₂ glasses and component bands assignments were shown in Tables 3 and 4, respectively.

According to the literature [70,77], the band at around 350 cm⁻¹ on the Raman spectra of the TP25BaF₂ and TP30BaF₂ glasses can be assigned to the bending vibration of P–F bonds. The bands at 460–440 cm⁻¹ and 660–650 cm⁻¹ on the spectra of all glasses are associated with bending vibration of Te–(O,F)–Te or O,F–Te–O,F bonds of [Te(O,F)₄] trigonal bipyramidal units [78] and stretching variation of Te–O, F bonds in [Te(O,F)₄] units, respectively [79]. The integral intensities of bands at 460–440 cm⁻¹ and 660–650 cm⁻¹ on the deconvoluted Raman spectra of glasses decreased with increasing BaF₂ content from 177 (TP5BaF₂) to 111 (TP30BaF₂) for band at 460–440 cm⁻¹, and from 204 (TP5BaF₂) to 66 (TP30BaF₂) for band at 660–650 (Table 3). It was due to reduction of the content of tellurite oxide at the expense of BaF₂ and/or transformation of the [Te(O,F)₄] units into [Te(O,F)₃] and [Te(O,F)₃₊₁] units. The presence of the [Te(O,F)₃] and [Te(O,F)₃₊₁] units in the network of glasses confirmed the presence of the bands at around 590–560 cm⁻¹ [80] and 790–770 cm⁻¹ [81]. The integral intensities of these bands have been changed with the addition of BaF₂ content, i.e. increased in BaF₂ amount caused accrual in the integral intensities of the bands at 590–560 cm⁻¹ from 39 (TP5BaF₂) to 153 (TP30BaF₂) and 790–770 cm⁻¹ from 83 (TP5BaF₂) to 144 (TP15BaF₂) and to 162 (TP30BaF₂) - Figs. 6b–d, Table 3. The increase in the integral intensities of the Raman bands with the addition of BaF₂ has been also noted for bands at 890–870 cm⁻¹ from 54 (TP5BaF₂) to 137 (TP30BaF₂) and 980–940 cm⁻¹ from 27 (TP5BaF₂) to 49 (TP15BaF₂)

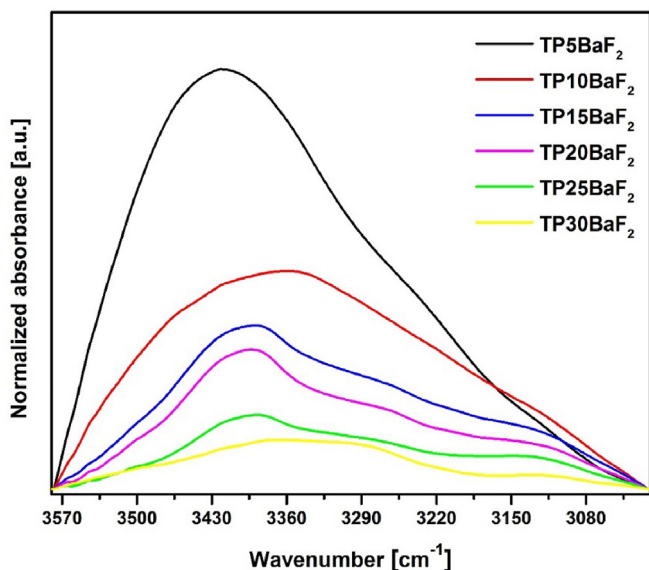


Fig. 5. MIR spectra in the $3600\text{--}3000\text{ cm}^{-1}$ range of glasses with varying BaF_2 content.

and to 87 (TP30BaF₂) - Figs. 6b–d, Table 3, corresponding to the symmetric stretching vibration of the P–F bonds [82] and symmetric stretching vibration of P(O,F)₄ in P⁰ units, respectively [83].

In the deconvoluted Raman spectra of the TP5BaF₂, TP15BaF₂, and TP30BaF₂ glasses (Figs. 6b–d) band at around $740/722/714\text{ cm}^{-1}$ is related to the Te(O,F)₄ tpb units [84], band at $1043/1035/1026\text{ cm}^{-1}$ can be attributed to the stretching vibrations of bridging P–O–P bonds in P¹ units [85], however band at $1099/1112/1120\text{ cm}^{-1}$ is associated with stretching vibrations of non-bridging bonds P(O,F)₄ of P² units [77], 88], (Figs. 6b–d, Tables 3 and 4).

As can be seen in Figs. 6b–d and in Table 3, the integral intensities of the bands corresponding to the symmetric stretching vibration of P(O,F)₄ in P⁰ units (band at $981/961/944\text{ cm}^{-1}$) and stretching vibrations of bridging P–O, F–P bonds in P¹ units (at $1043/1035/1026\text{ cm}^{-1}$), increased with addition of the BaF₂ from 27 (TP5BaF₂) to 49 (TP15BaF₂) and to 87 (TP30BaF₂), as well as from 10 (TP5BaF₂) to 16 (TP15BaF₂) and 24 (TP30BaF₂), respectively. However, the integral intensity of the band at $1097/1112/1120\text{ cm}^{-1}$ related to the stretching vibrations of non-bridging bonds P(O,F)₄ of P² units decreased from 4 (TP5BaF₂) to 3 (TP15BaF₂) and 1 (TP30BaF₂). Thus an increase in the content of barium ions in the network of all glasses caused an increase in the number of P¹ and P⁰

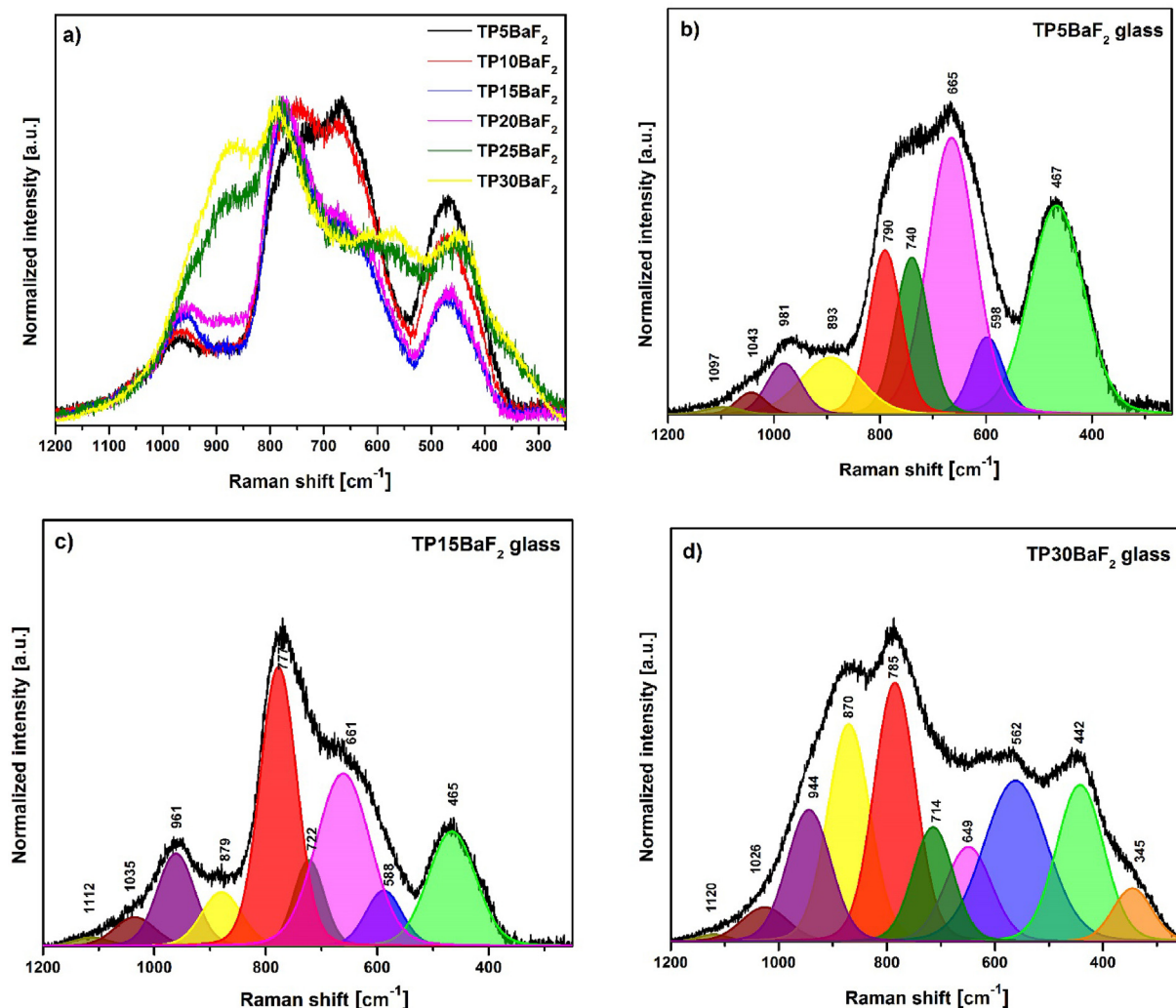


Fig. 6. Raman spectra in the $1200\text{--}300\text{ cm}^{-1}$ range of glasses with varying BaF_2 content a) and deconvoluted Raman spectra of TP5BaF₂ b), TP15BaF₂ c) and TP30BaF₂ d) glasses.

Table 3
Raman spectroscopy spectral fitting parameters spectra of TP5BaF₂, TP15BaF₂, and TP30BaF₂ glasses.

TP5BaF ₂ glass		
Peak [cm ⁻¹] (±2.0)	Integral intensity (±0.5)	FWHM [cm ⁻¹] (±2.0)
467	177	121
598	39	72
665	204	105
740	81	74
790	83	72
893	54	135
981	27	77
1043	10	65
1097	4	80
TP15BaF ₂ glass		
Peak [cm ⁻¹] (± 2.0)	Integral intensity (± 0.5)	FWHM [cm ⁻¹] (± 2.0)
466	77	101
588	28	76
661	132	115
722	37	64
777	144	78
879	30	84
961	49	79
1035	16	86
1112	3	73
TP30BaF ₂ glass		
Peak [cm ⁻¹] (± 2.0)	Integral intensity (± 0.5)	FWHM [cm ⁻¹] (± 2.0)
345	31	86
442	111	103
562	153	138
649	66	101
714	69	88
785	162	91
870	137	92
944	87	96
1026	24	102
1120	1	63

units at the expense of P² units. Simultaneously, the tellurium subnetwork of the glasses was also depolymerized. It has been confirmed by an increase in the integral intensities of the bands at around 590–560 cm⁻¹ (band due to Te–O, F–Te stretching vibration in [Te(O,F)₃] trigonal pyramids and [Te(O,F)₃₊₁] units) from 39 (TP5BaF₂) to 153 (TP30BaF₂), and 790 cm⁻¹ (band related to Te–(O,F) stretching vibration in [Te(O,F)₃] trigonal pyramids or symmetric stretching vibration in [Te(O,F)₃₊₁] units) from 83 (TP5BaF₂) to 144 (TP15BaF₂) and to 162 (TP30BaF₂). Additionally, the decrease in the integral intensities of the bands: at around 460–440 cm⁻¹ (band associated with bending vibration of Te–(O,F)–Te or O,F–Te–O,F bands of [Te(O,F)₄] trigonal bipyramidal units from 177 (TP5BaF₂) to 111 (TP30BaF₂) and band at 660–640 cm⁻¹ (band related to stretching variation of Te–O,F in [Te(O,F)₄] units) from 204 (TP5BaF₂) to 132 (TP15BaF₂) and to 66 (TP30BaF₂) has been observed – Table 3. Depolymerization of the phosphate-tellurite network of the glasses due to an increase in BaF₂ content resulted in shifting the position of the component bands in the Raman spectra of glasses towards lower wavenumbers – Figs. 6b–d.

Raman spectroscopy study of the glasses is consistent with the MIR results. However, based on the Raman spectra of glasses, it has been additionally demonstrated that due to an increase in the amount of BaF₂ into the chemical composition of glasses, not only phosphate network but also the tellurite network of glasses has been depolymerized.

In Fig. 7a, the ³¹P MAS NMR spectra of all glasses were presented. Each spectrum was characterized by a resonance signal (peak) in the +30 to –30 ppm range. With the BaF₂ addition, the position of the peak on spectra of the glasses has been shifted

Table 4
Band assignment.

Band position [cm ⁻¹]	Assignment
–/–/345	Bending vibration of O–P–O bonds [77]
467/465/442	bending vibration of Te–(O, F)–Te or O, F–Te–O, F bands of [Te(O, F) ₄] trigonal bipyramidal units [78]
598/588/562	Te–O, F–Te stretching vibration in [Te(O, F) ₃] trigonal pyramids and [Te(O, F) ₃₊₁] units [80]
665/661/649	stretching variation of Te–O, F bonds in [Te(O, F) ₄] units [79]
740/722/714	Bands assigned to the Te(O, F) ₄ tbp units [83]
790/777/785	Te–(O, F) stretching vibration in [Te(O, F) ₃] trigonal pyramids or symmetric stretching vibration in [Te(O, F) ₃₊₁] units [81]
893/879/870	symmetric stretching vibration of the P–F bonds [82]
981/961/944	symmetric stretching vibration of P(O, F) ₄ in P ⁰ units [83]
1043/1035/1026	stretching vibrations of bridging P–O, F–P bonds in P ¹ units [85]
1097/1112/1120	stretching vibrations of non-bridging bonds P(O, F) ₄ of P ² units [77,85]

towards higher resonance frequencies, i.e. from –4 ppm on the spectrum of TeP5BaF₂ glass to 0 ppm on the spectrum of the TeP30BaF₂ glass (Fig. 7a). On the basis of the detailed analysis of the deconvoluted peak parameters of the ³¹P MAS NMR spectra of glasses, it is possible to obtain the fractional areas of all the P⁽ⁿ⁾_mTe units, where n corresponds with coordination number of the phosphorus atoms and m is associated with bridging ions of the P–(O, F)–Te in the glass network, respectively [86,87]. This information was presented in Figs. 7b–d and Table 5 for TP5BaF₂, TP15BaF₂, and TP30BaF₂ glasses.

Based on deconvoluted ³¹P MAS NMR spectra of the glasses, P²_{2Te}, P²_{1Te}, P²_{0Te}, P¹_{1Te}, and P⁰ units were detected (Table 5) [86,87]. Additionally, it was found that the amount of the P²_{1Te}, P²_{0Te} species decreased in the network of glasses with an increase in the amount of BaF₂. Reduction in the number of P² units caused an increase in the number of P¹_{1Te}, P⁰ species (Figs. 7b–d and Table 5). Compositional variation of relative fractions of various phosphate species derived from ³¹P MAS NMR has been presented in Fig. 8. The changes in the ³¹P MAS NMR spectra are related to the depolymerization of the glasses network.

Based on analysis of ³¹P MAS NMR spectra of the glasses have been found that barium ions depolymerized primarily P²_{1Te}, P²_{0Te} units in the network of the oxyfluoride phosphate-tellurite glasses.

4. Conclusions

The structure of the oxyfluoride phosphate-tellurite glasses in the system of the (69.5–x)TeO₂–10P₂O₅–xBaF₂–20(ZnF₂–Na₂O)–0.5ErF₃ x = 5, 10, 15, 20, 25, 30 mol % were investigated. From the XRD study, the amorphous nature of glass samples was confirmed. Based on the results from the deconvoluted MIR and Raman spectra of the glasses was found that networks of all glasses are created by Te(O,F)₄, Te(O,F)₃, Te(O,F)₃₊₁, P², P¹ and P⁰ units. The increase in the BaF₂ content resulted in the conversion of Te(O,F)₄ into Te(O,F)₃, Te(O,F)₃₊₁ units, as well as P² into P¹ and P⁰ units. Additionally, P²_{2Te}, P²_{1Te}, P²_{0Te}, P¹_{1Te}, units were detected (³¹P MAS NMR study) in the network of glasses. From ³¹P MAS NMR spectra of the glasses has been found that barium ions depolymerized primarily P²_{1Te}, P²_{0Te} units in the phosphate subnetwork of glasses. The changes in the MIR, Raman and ³¹P MAS NMR spectra were related to the depolymerization of the glasses network with the increase in the BaF₂ content. The addition of the BaF₂ led to a decrease in the OH free group.

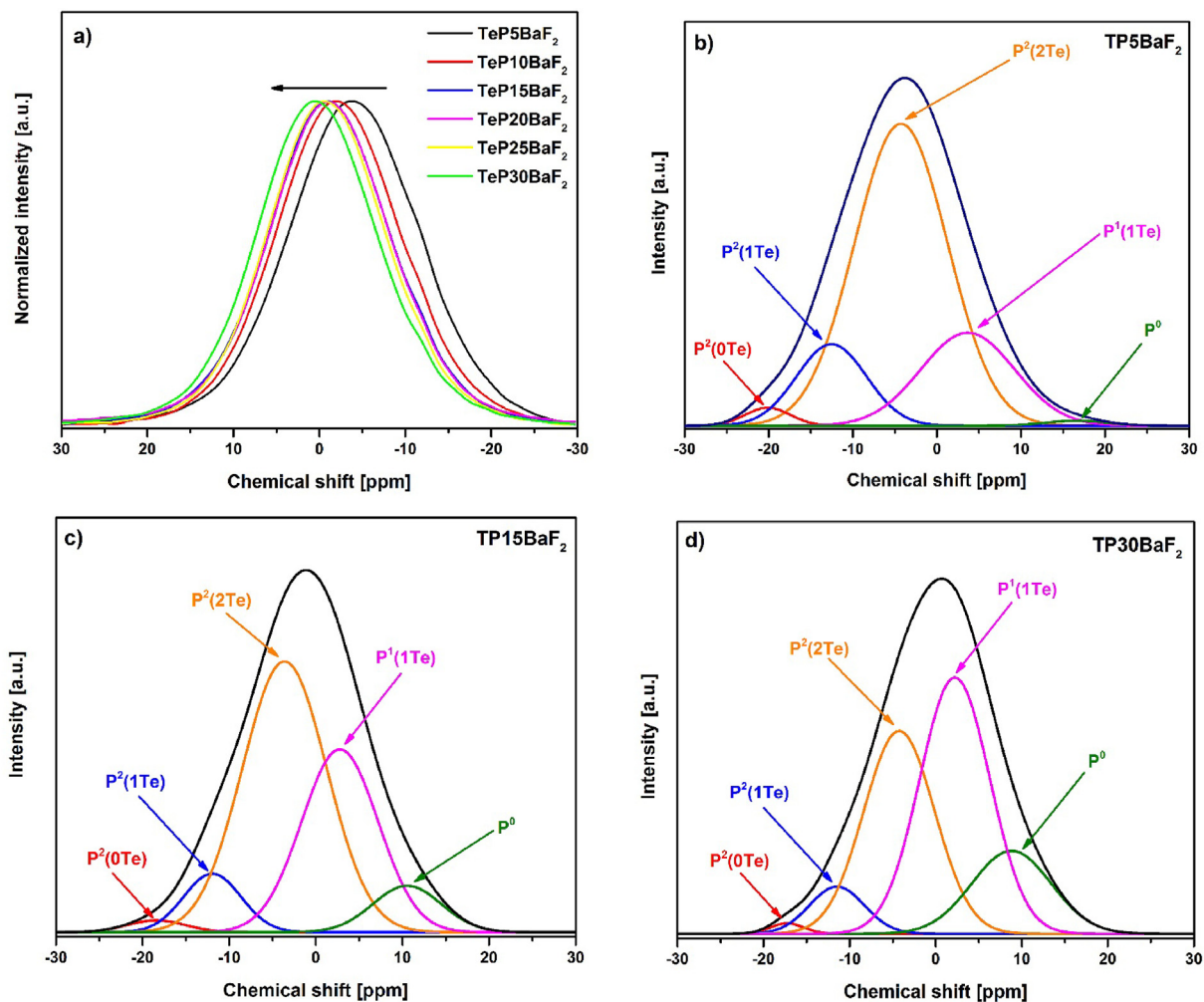


Fig. 7. ^{31}P MAS NMR spectra of glasses with varying BaF_2 content a) and deconvoluted ^{31}P MAS NMR spectra of TP5BaF₂ b), TP15BaF₂ c) and TP30BaF₂ d) glasses.

Table 5

Deconvolution of the ^{31}P MAS NMR spectra of the TP5BaF₂, TP15BaF₂, and TP30BaF₂ glasses.

Glass	Phosphorus species	Position [ppm] (± 0.5)	Relative fraction [%] (± 1.0)	FWHM [ppm] (± 0.5)
TP5BaF ₂	P ² _{2Te}	-20	2	6
	P ² _{1Te}	-13	13	10
	P ² _{0Te}	-4	64	13
	P ¹ _{1Te}	4	20	13
	P ⁰	17	1	8
TP15BaF ₂	P ² _{2Te}	-18	2	8
	P ² _{1Te}	-12	8	8
	P ² _{0Te}	-4	52	11
	P ¹ _{1Te}	3	32	10
	P ⁰	11	7	9
TP30BaF ₂	P ² _{2Te}	-17	2	5
	P ² _{1Te}	-11	6	7
	P ² _{0Te}	-4	34	10
	P ¹ _{1Te}	2	42	10
	P ⁰	9	16	11

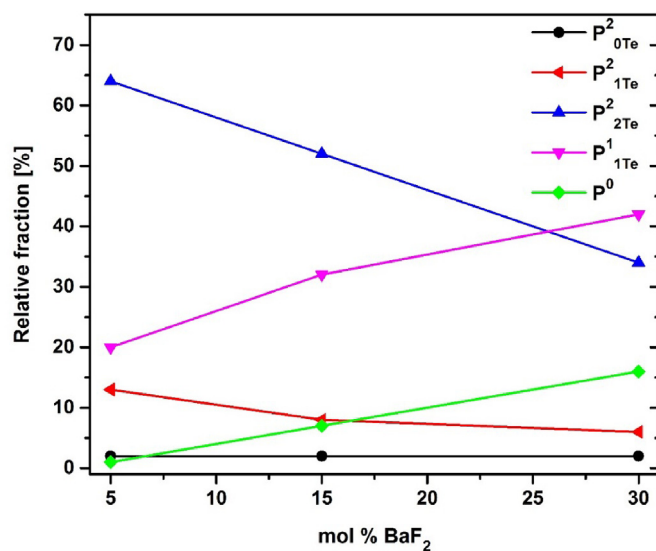


Fig. 8. Compositional variation of relative fractions of various phosphate species derived from ^{31}P MAS NMR spectra of glasses.

Declaration of competing interest

The authors declare that they have no known competing financial interests or personal relationships that could have appeared to influence the work reported in this paper.

CRediT authorship contribution statement

M. Lesniak: Writing - original draft, Writing - review & editing. **G. Mach:** Writing - original draft, Writing - review & editing. **B. Starzyk:** Writing - original draft, Writing - review & editing. **A. Baranowska:** Writing - original draft, Writing - review & editing. **M. Bik:** Writing - original draft, Writing - review & editing. **M. Kochanowicz:** Writing - original draft, Writing - review & editing. **J. Zmojda:** Writing - original draft, Writing - review & editing. **P. Miluski:** Writing - original draft, Writing - review & editing. **M. Sitarz:** Writing - original draft, Writing - review & editing. **D. Dorosz:** Writing - original draft, Writing - review & editing.

Acknowledgment

The research activity was granted by the National Science Centre, Poland No. 2016/23/B/ST8/00706.

References

- [1] Z. He, C. Zhu, S. Huang, X. Wu, Luminescent properties of Pr³⁺ and Tm³⁺ doped oxyfluoride silicate glasses for light emitting diode applications, *Vacuum* 159 (2008) 269–276, <https://doi.org/10.1016/j.vacuum.2018.10.048>.
- [2] E.F. Huerta, A.N. Meza-Rocha, R. Lozada-Morales, A. Speghini, S. Bordignon, U. Caldiño, White, Yellow and reddish-orange light generation in lithium-aluminum-zinc phosphate glasses co-doped with Dy³⁺/Tb³⁺ and tri-doped with Dy³⁺/Tb³⁺/Eu³⁺, *J. Lumin.* 219 (2020) 116882, <https://doi.org/10.1016/j.jlumin.2019.116882>.
- [3] C. Yu, X. Zhang, X. Li, J. Zhang, S. Xu, X. Zhang, Y. Zhang, X. Wang, Li Wang, G. Sui, B. Chen, Determination of Judd-Ofelt parameters for Eu³⁺-doped alkali borate glasses, *Mater. Res. Bull.* 120 (2019) 110590, <https://doi.org/10.1016/j.matresbull.2019.110590>.
- [4] M. Kochanowicz, J. Zmojda, P. Miluski, A. Baranowska, T. Ragin, J. Dorosz, M. Kuwik, W.A. Pisarski, J. Pisarska, M. Leśniak, D. Dorosz, 2 μm emission in gallo-germanate glasses and glass fibers co-doped with Yb³⁺/Ho³⁺ and Yb³⁺/Tm³⁺/Ho³⁺, *J. Lumin.* 211 (2019) 341–346, <https://doi.org/10.1016/j.jlumin.2019.03.060>.
- [5] K. Suresh, C.K. Jayasankar, Conversion of blue-green photon into NIR photons in Ho³⁺/Yb³⁺ co-doped zinc tellurite glasses, *J. Alloys Compd.* 788 (2019) 1048–1055, <https://doi.org/10.1016/j.jallcom.2019.02.258>.
- [6] Y. Zhu, H. Shen, M. Zhou, X. Su, J. Li, G. Yang, H. Shao, Y. Zhou, 2.0 μm band emission enhancement and energy transfer in Ho³⁺/Yb³⁺/Er³⁺ tri-doped tellurite glasses, *J. Lumin.* 210 (2019) 28–37, <https://doi.org/10.1016/j.jlumin.2019.02.015>.
- [7] M. Seshadri, M.J.V. Bell, V. Anjos, Y. Messaddeq, Spectroscopic investigations on Yb³⁺ doped and Pr³⁺/Yb³⁺ codoped tellurite glasses for photonic applications, *J. Rare Earths* (2020), <https://doi.org/10.1016/j.jre.2019.12.006>. In press.
- [8] W. Fu, C. Zhang, G. Hou, J. Xia, G. Li, Y. Ping, Enhanced fluorescence emission of 2.7 μm from high thermal stability Er³⁺/Bi³⁺ co-doped tellurite glasses for mid-infrared lasers, *Optik* 182 (2019) 308–313, <https://doi.org/10.1016/j.ijleo.2019.01.034>.
- [9] K. Pach, E. Golis, El S. Yousef, M. Sitarz, J. Filipiecki, Structural studies of tellurite glasses doped with erbium ions, *J. Mol. Struct.* 182 (2019) 308–313, <https://doi.org/10.1016/j.jle.2019.01.034>.
- [10] E.A. Anashkina, A.V. Andrianov, V.V. Dorofeev, A.V. Kima, V.V. Koltashev, G. Leuchs, S.E. Motorinb, S.V. Muravyev, A.D. Plekhovich, Development of infrared fiber lasers at 1555 nm and at 2800 nm based on Er-doped zinc-tellurite glass fiber, *J. Non-Cryst. Sol.* 525 (2019) 119667, <https://doi.org/10.1016/j.jnoncrysol.2019.119667>.
- [11] J. Lie, X. Xiao, S. Gu, Y. Xu, Z. Zhou, H. Guo, Preparation and optical properties of TeO₂-BaO-ZnO-ZnF₂ fluoro-tellurite glass for mid-infrared fiber Raman laser applications, *Opt. Mater.* 66 (2017) 567–572, <https://doi.org/10.1016/j.optmat.2017.03.006>.
- [12] M.P. Smayev, V.V. Dorofeev, A.N. Moiseev, A.G. Okhrimchuk, Femtosecond laser writing of a depressed cladding single mode channel waveguide in high-purity tellurite glass, *J. Non-Cryst. Sol.* 480 (2018) 100–106, <https://doi.org/10.1016/j.jnoncrysol.2017.11.007>.
- [13] J.J. Leal, R. Narro-García, J.P. Flores-De los Ríos, N. Gutierrez-MendezVictor, H. Ramos-Sánchez, J.R. González-Castillo, E. Rodríguez, Effect of TiO₂ on the thermal and optical properties of Er³⁺/Yb³⁺ co-doped tellurite glasses for

- optical sensor, *J. Lumin.* 208 (2019) 342–349, <https://doi.org/10.1016/j.jlumin.2019.01.004>.
- [14] Y. Zhang, Z. Xiao, H. Lei, L. Zeng, J. Tang, Er³⁺/Yb³⁺ co-doped tellurite glasses for optical fiber thermometry upon UV and NIR excitations, *J. Lumin.* 212 (2019) 61–68, <https://doi.org/10.1016/j.jlumin.2019.04.021>.
- [15] V. Krishnaiah, P. Venkatalakshamma, Ch Basavapoornima, I.R. Martín, K. Soler-Carracedo, M.A. Hernández-Rodríguez, V. Venkatramu, C.K. Jayasankar, Er³⁺-doped tellurite glasses for enhancing a solar cell photocurrent through photon upconversion upon 1500 nm excitation, *Mater. Chem. Phys.* 199 (2017) 67–72, <https://doi.org/10.1016/j.materchemphys.2017.06.003>.
- [16] M.M. Taniguchi, V.S. Zanuto, P.N. Portes, L.C. Malacarne, N.G. Castelli Astrath, J.D. Marconi, M.P. Belançon, Glass engineering to enhance Si solar cells: a case study of Pr³⁺-Yb³⁺ codoped tellurite-tungstate as spectral converter, *J. Non-Cryst. Sol.* 526 (2019) 119717, <https://doi.org/10.1016/j.jnoncrysol.2019.119717>.
- [17] S. Nandyala, P. Gomes, G. Hungerford, L. Grenho, M.H. Fernandez, A. Stamboulis, Development of bioactive tellurite-lanthanide ions-reinforced hydroxyapatite composites for biomedical and luminescence applications, in: R. El-Mallawany (Ed.), *Tellurite Glass Smart Materials*, first ed., Springer, 2018, pp. 275–288.
- [18] P. Sailaja, Sk Mahamuda, Rupesh A. Talewar, K. Swapna, A.S. Rao, Spectroscopic investigations of dysprosium ions doped oxy chloro boro tellurite glasses for visible photonic device applications, *J. Alloys Compd.* 789 (2019) 744–754, <https://doi.org/10.1016/j.jallcom.2019.03.148>.
- [19] S. Polosan, Structure and low field magnetic properties in phosphate-tellurite glasses, *J. Non-Cryst. Solids.* 524 (2019) 119651, <https://doi.org/10.1016/j.jnoncrysol.2019.119651>.
- [20] L. Hu, D. He, H. Chen, X. Wang, T. Meng, L. Wen, J. Hu, Y. Xu, Sh Li, Y. Chen, W. Chen, Sh Chen, J. Tang, B. Wang, Research and development of neodymium phosphate laser glass for high power laser application, *Opt. Mater.* 63 (2017) 213–220, <https://doi.org/10.1016/j.optmat.2016.11.052>.
- [21] Ch Basavapoornima, T. Maheswari, Shobha Rani Depuru, C.K. Jayasankar, Sensitizing effect of Yb³⁺ ions on photoluminescence properties of Er³⁺ ions in lead phosphate glasses: optical fiber amplifiers, *Opt. Mater.* 86 (2018) 256–269, <https://doi.org/10.1016/j.optmat.2018.09.027>.
- [22] N. Luewasirikul, N. Chanthim, Y. Tariwong, J. Kaewkhao, Erbium-doped calcium barium phosphate glasses for 1.54 μm broadband optical amplifier, *Mater. Today: proceed.* 5 (2018) 14009–14016, <https://doi.org/10.1016/j.matpr.2018.02.053>.
- [23] L. Hao, M. Pei, T. Yang, C. Ming, Double-sensitivity temperature sensor based on excitation intensity ratio of Eu³⁺ doped phosphate glass ceramic, *Optik* 204 (2020) 164188, <https://doi.org/10.1016/j.ijleo.2020.164188>.
- [24] M.R. Dousti, G.Y. Poirierb, S.S. de Camargo, Tungsten sodium phosphate glasses doped with trivalent rare earth ions (Eu³⁺, Tb³⁺, Nd³⁺ and Er³⁺) for visible and near-infrared applications, *J. Non-Cryst. Sol.* 530 (2020) 119838, <https://doi.org/10.1016/j.jnoncrysol.2019.119838>.
- [25] V.M. Martins, G.A. Azevedo, A.A. Andrade, D.N. Messias, A.F.G. do Monte, N.O. Dantas, V. Pilla, T. Catunda, A. Braud, R. Moncorgé, Spatial and temporal observation of energy transfer processes in Pr-doped phosphate glasses, *Opt. Mater.* 37 (2014) 387–390, <https://doi.org/10.1016/j.optmat.2014.06.031>.
- [26] Y. Chen, G. Chen, X. Liu, C. Yuan, C. Zhou, Tunable luminescence mediated by energy transfer in Tm³⁺/Dy³⁺ co-doped phosphate glasses under UV excitation, *Opt. Mater.* 73 (2017) 535–540, <https://doi.org/10.1016/j.optmat.2017.09.011>.
- [27] A. Górny, M. Sołtys, J. Pisarska, W.A. Pisarski, Effect of acceptor ions concentration in lead phosphate glasses co-doped with Tb³⁺-Ln³⁺ (Ln = Eu, Sm) for LED applications, *J. Rare Earths* 37 (2019) 1145–1151, <https://doi.org/10.1016/j.jre.2019.02.005>.
- [28] B. Nagaraja Naick, S. Damodaraiah, V. Reddy Prasad, R.P. Vijaya Lakshmi, Y.C. Ratnakaram, Judd-Ofelt analysis and luminescence studies on Dy³⁺-doped different phosphate glasses for white light emitting material applications, *Optik* 192 (2019) 162980, <https://doi.org/10.1016/j.ijleo.2019.162980>.
- [29] P. Mošner, K. Vosejpková, L. Koudelka, L. Montagne, B. Revel, Structure and properties of glasses in ZnO-P₂O₅-TeO₂ system, *J. Non-Cryst. Sol.* 357 (2011) 2648–2652, <https://doi.org/10.1016/j.jnoncrysol.2010.12.052>.
- [30] El S. Yousef, B. Al-Qaisi, Kinetics and fabrication nanocrystallization of optical tellurophosphate glasses in system as: TeO₂-P₂O₅-ZnO-LiNbO₃, *J. Alloys Compd.* 538 (2012) 193–200, <https://doi.org/10.1016/j.jallcom.2012.05.088>.
- [31] E. Golis, ElS. Yousef, M. Reben, K. Kotynia, J. Filipiecki, Measurements of defect structures by positron annihilation lifetime spectroscopy of the tellurite glass TeO₂-P₂O₅-ZnO-LiNbO₃ doped with ions of rare earth elements: Er³⁺, Nd³⁺ and Gd³⁺, *Solid State Sci.* 50 (2015) 81–84, <https://doi.org/10.1016/j.solidstatosciences.2015.10.017>.
- [32] M.M. Elkholy, L.M. Sharaf, El-Deen, The dielectric properties of TeO₂-P₂O₅ glasses, *Mater. Chem. Phys.* 65 (2000) 192–196, [https://doi.org/10.1016/S0254-0584\(00\)00243-1](https://doi.org/10.1016/S0254-0584(00)00243-1).
- [33] K. Linganna, R. Narro-García, H. Desirena, E. De la Rosa, Ch Basavapoornima, V. Venkatramu, C.K. Jayasankar, Effect of P₂O₅ addition on structural and luminescence properties of Nd³⁺-doped tellurite glasses, *J. Alloys Compd.* 684 (2016) 322–327, <https://doi.org/10.1016/j.jallcom.2016.05.082>.
- [34] P. Nandi, G. Jose, Erbium doped phospho-tellurite glasses for 1.5 μm optical amplifiers, *Optic Commun.* 265 (2006) 588–593, <https://doi.org/10.1016/j.optcom.2006.03.045>.
- [35] M. Irannejad, G. Jose, A. Jha, D.P. Steenson, A parametric study of Er³⁺-ions

- doped Phospho-tellurite glass thin films by pulsed laser deposition, *Opt. Mater.* 33 (2010) 215–219, <https://doi.org/10.1016/j.optmat.2010.08.017>.
- [36] A. Abdel-Kader, R. El-Mallawany, M. Elkholy, H. Farag, Thermoluminescence dosimetry of rare-earth doped tellurite phosphate glasses, *Mater. Chem. Phys.* 36 (1994) 365–370, [https://doi.org/10.1016/0254-0584\(94\)90056-6](https://doi.org/10.1016/0254-0584(94)90056-6).
- [37] P. Nandi, G. Jose, Spectroscopic properties of Er³⁺ doped phospho-tellurite glasses, *Phys. B Condens. Matter* 381 (2006) 66–72, <https://doi.org/10.1016/j.physb.2005.12.255>.
- [38] P. Nandi, G. Jose, Superfluorescence from Yb- and Yb–Er-doped phospho-tellurite glass fibres, *Opt. Fiber Technol.* 14 (2008) 275–280, <https://doi.org/10.1016/j.yofte.2008.01.004>.
- [39] Y. Yang, Z. Yang, P. Lia, X. Li, Q. Guo, B. Chen, Dependence of optical properties on the composition in Er³⁺-doped xNaPO₃–(80–x)TeO₂–10ZnO–10Na₂O glasses, *Opt. Mater.* 32 (2009) 133–138, <https://doi.org/10.1016/j.optmat.2009.06.016>.
- [40] S. Rada, E. Culea, FTIR spectroscopic and DFT theoretical study on structure of europium–phosphate–tellurate glasses and glass ceramics, *J. Mol. Struct.* 929 (2009) 141–148, <https://doi.org/10.1016/j.molstruc.2009.04.021>.
- [41] Y. Yang, W. Zhang, S. Guo, Z. Yang, Compositional dependence of up-conversion emission and optical transition in Yb³⁺–Ho³⁺ codoped tellurite-phosphate glasses, *Proceed.* 7749 (2010) 77490E, <https://doi.org/10.1117/12.869470>.
- [42] I. Jlassi, H. Elhouichet, M. Ferid, C. Barthou, Judd–Ofelt analysis and improvement of thermal and optical properties of tellurite glasses by adding P₂O₅, *J. Lumin.* 130 (2010) 2394–2401, <https://doi.org/10.1016/j.jlumin.2010.07.026>.
- [43] T. Cheng, Y. Sakai, T. Suzuki, Y. Ohishi, Fabrication and characterization of an all-solid tellurite–phosphate photonic bandgap fiber, *Opt. Lett.* 40 (2015) 2088–2090, <https://doi.org/10.1364/OL.40.002088>.
- [44] K. Linganna, R. Narro-García, H. Desirena, E. De la Rosa, Ch Basavapooranima, V. Venkatramu, C.K. Jayasankar, Effect of P₂O₅ addition on structural and luminescence properties of Nd³⁺-doped tellurite glasses, *J. Alloys Compd.* 684 (2016) 322–327, <https://doi.org/10.1016/j.jallcom.2016.05.082>.
- [45] I. Jlassi, H. Fares, H. Elhouichet, Enhancement of spectroscopic and luminescence properties of Er³⁺ doped tellurite glasses by adding P₂O₅ for lasing materials, *J. Lumin.* 194 (2018) 569–578, <https://doi.org/10.1016/j.jlumin.2017.09.012>.
- [46] M. Ennouri, I. Jlassi, E. Habib, G. Bernard, Improvement of spectroscopic properties and luminescence of Er³⁺ ions in phospho-tellurite glass ceramics by formation of ErPO₄ nanocrystals, *J. Lumin.* 216 (2019) 116753, <https://doi.org/10.1016/j.jlumin.2019.116753>.
- [47] N. Elkhoshkhany, M. Mahmoud, E. S. Yousef, Structural, thermal and optical properties of novel oxyfluorotellurite glasses, *Chalcogenide Lett.* 16 (2019) 265–282.
- [48] M. Lesniak, J. Zmojda, M. Kochanowicz, P. Miluski, A. Baranowska, G. Mach, M. Kuwik, J. Pisarska, W.A. Pisarski, D. Dorosz, *Materials* 12 (2019) 3429, <https://doi.org/10.3390/ma12203429>.
- [49] F. Chen, T. Wei, X. Jing, Y. Tian, J. Zhang, S. Xu, Investigation of mid-infrared emission characteristics and energy transfer dynamics in Er³⁺ doped oxy-fluoride tellurite glass, *Sci. Rep.* 5 (2015) 10676, <https://doi.org/10.1038/srep10676>.
- [50] D. Rajesh, M.R. Dousti, R.J. Amjad, A.S.S. de Camargo, Enhancement of down- and upconversion intensities in Er³⁺/Yb³⁺ co-doped oxyfluoro tellurite glasses induced by Ag species and nanoparticles, *J. Lumin.* 192 (2017) 250–255, <https://doi.org/10.1016/j.jlumin.2017.06.059>.
- [51] B. Kliemesz, R. Lisiecki, W. Ryba-Romanowski, Thermosensitive Tm³⁺/Yb³⁺ co-doped oxyfluorotellurite glasses – spectroscopic and temperature sensor properties, *J. Alloys Compd.* 823 (2020) 153753, <https://doi.org/10.1016/j.jallcom.2020.153753>.
- [52] Y. Wang, C. Xu, Z. Zhang, C. Zheng, J. Pei, L. Sun, Enhanced 1–5 μm near- and mid-infrared emission in Ho³⁺/Yb³⁺ codoped TeO₂–ZnF₂ oxyfluorotellurite glasses, *J. Rare Earths* (2019), <https://doi.org/10.1016/j.jre.2019.10.008>. In press.
- [53] Z. Zhang, C. Xu, B. Huang, Y. Wang, J. Pei, C. Zheng, L. Sun, Increasing ZnF₂ content enhancing the near- and mid-infrared emission in Er³⁺/Yb³⁺ codoped oxyfluorotellurite glasses with decreased hydroxyl, *J. Lumin.* 216 (2019) 116683, <https://doi.org/10.1016/j.jlumin.2019.116683>.
- [54] M. Leśniak, R. Szal, B. Starzyk, M. Gajek, M. Kochanowicz, J. Zmojda, P. Miluski, J. Dorosz, M. Sitarz, D. Dorosz, Influence of barium oxide on glass-forming ability and glass stability of the tellurite–phosphate oxide glasses, *J. Therm. Anal. Calorim.* 138 (2019) 4295–4302, <https://doi.org/10.1007/s10973-019-08715-6>.
- [55] H. Gangwar, V. Singh, B.S. Tewari, H. Gupta, L.P. Purohit, Study of zinc doped tellurite glasses using XRD, UV–Vis and FTIR, *Mater. Today: proceed.* 17 (2019) 329–337, <https://doi.org/10.1016/j.matpr.2019.06.437>.
- [56] N. Gupta, Hirdesh, R. Kaur, A. Khanna, S. Singh, B.K. Gupta, Spatially resolved X-ray fluorescence, Raman and photoluminescence spectroscopy of Eu³⁺/Er³⁺ doped tellurite glasses and anti-glasses, *J. Non-Cryst. Sol.* 513 (2019) 24–35, <https://doi.org/10.1016/j.jnoncrysol.2019.01.039>.
- [57] L.Y. Mao, J.L. Liu, L.X. Li, W.C. Wang, TeO₂–Ga₂O₃–ZnO ternary tellurite glass doped with Tm³⁺ and Ho³⁺ for 2 μm fiber lasers, *J. Non-Cryst. Sol.* 531 (2020) 119855, <https://doi.org/10.1016/j.jnoncrysol.2019.119855>.
- [58] A. Kaur, Hirdesh, A. Khanna, M. Fábán, P.S.R. Krishna, A.B. Shinde, Structure of lead tellurite glasses and its relationship with stress-optic properties, *Mater. Res. Bull.* 110 (2019) 239–246, <https://doi.org/10.1016/j.materresbull.2018.10.008>.
- [59] D. Holland, J. Bailey, G. Ward, B. Turner, P. Tierney, R. Dupree, ¹²⁵Te and ²³Na NMR investigation of the structure and crystallisation of sodium tellurite glasses, *Solid State Nucl. Magn. Reson.* 27 (2005) 16–27, <https://doi.org/10.1016/j.ssnmr.2004.06.010>.
- [60] E.R. Barney, A.C. Hannon, D. Holland, N. Umetsaki, M. Tatsumisago, Alkali environments in tellurite glasses, *J. Non-Cryst. Sol.* 414 (2015) 33–41, <https://doi.org/10.1016/j.jnoncrysol.2015.01.023>.
- [61] Z. Whittles, M. Marple, I. Hung, Z. Gan, S. Sen, Structure of BaO–TeO₂ glasses: a two-dimensional ¹²⁵Te NMR spectroscopic study, *J. Non-Cryst. Sol.* 481 (2018) 282–288, <https://doi.org/10.1016/j.jnoncrysol.2017.10.055>.
- [62] J.C. McLaughlin, S.L. Tagg, J.W. Zwanziger, D.R. Haeffner, S.D. Shastri, The structure of tellurite glass: a combined NMR, neutron diffraction, and X-ray diffraction study, *J. Non-Cryst. Sol.* 274 (2000) 1–8, [https://doi.org/10.1016/S0022-3093\(00\)00199-X](https://doi.org/10.1016/S0022-3093(00)00199-X).
- [63] A.G. Kalampounias, N.K. Nasikas, G.N. Papatheodorou, Structural investigations of the xTeO–(1–x)GeO (x=0, 0.2, 0.4, 0.6, 0.8 and 1) tellurite glasses: a composition dependent Raman spectroscopic study, *J. Phys. Chem. Solid.* 72 (2011) 1052, <https://doi.org/10.1016/j.jpccs.2011.05.016>.
- [64] R.K. Brow, Review: the structure of simple phosphate glasses, *J. Non-Cryst. Sol.* 263–264 (2000) 1–28, [https://doi.org/10.1016/S0022-3093\(99\)00620-1](https://doi.org/10.1016/S0022-3093(99)00620-1).
- [65] H. Li, J. Yi, Z. Qin, Z. Sun, T. Xu, C. Wang, F. Zhao, Y. Hao, Z. Liang, Structures, thermal expansion, chemical stability and crystallization behavior of phosphate-based glasses by influence of rare earth, *J. Non-Cryst. Solids* 522 (2019) 119602, <https://doi.org/10.1016/j.jnoncrysol.2019.119602>.
- [66] R. Rajeswari, S. Surendra Babu, C.K. Spectroscopic characterization of alkali modified zinc-tellurite glasses doped with neodymium, *Spectrochim. Acta Mol. Biomol. Spectrosc.* 77 (2010) 134–140, <https://doi.org/10.1016/j.saa.2010.04.040>.
- [67] T. Djouama, M. Poulain, B. Bureau, R. Lebullenger, Structural investigation of fluorphosphates glasses by ¹⁹F, ³¹P MAS NMR and IR spectroscopy, *J. Non-Cryst. Sol.* 414 (2015) 16–20, <https://doi.org/10.1016/j.jnoncrysol.2015.01.017>.
- [68] N. Elkhoshkhany, H.M. Mohamed, UV–Vis–NIR spectroscopy, structural and thermal properties of novel oxyhalide tellurite glasses with composition TeO₂–B₂O₃–SrCl₂–LiF–Bi₂O₃ for optical application, *Respir. Physiol.* 13 (2019) 102222, <https://doi.org/10.1016/j.rinp.2019.102222>.
- [69] R.A.H. El-Mallawany, *Tellurite Glasses Handbook*, CRC Press, Washington, DC, USA, 2002.
- [70] D. Möncke, H. Eckert, Review on the structural analysis of fluoride-phosphate and fluoro-phosphate glasses, *J. Non-Cryst. Sol.* X 3 (2019) 100026, <https://doi.org/10.1016/j.nocx.2019.100026>.
- [71] O. Kibrishli, A.E. Ersundu, M. Çelikbilek Ersundu, Dy³⁺ doped tellurite glasses for solid-state lighting: an investigation through physical, thermal, structural and optical spectroscopy studies, *J. Non-Cryst. Sol.* 513 (2019) 125–136, <https://doi.org/10.1016/j.jnoncrysol.2019.03.020>.
- [72] W. Liu, J. Sanz, C. Pecharróman, I. Sobrados, S. Lopez-Esteban, R. Torrecillas, D.Y. Wang, J.S. Moya, B. Cabai, Synthesis, characterization and applications of low temperature melting glasses belonging to P₂O₅–CaO–Na₂O system, *Ceram. Int.* 45 (2019) 12234–12242, <https://doi.org/10.1016/j.ceramint.2019.03.133>.
- [73] S. Babu, M. Seshadri, P.V. Reddy, Y.C. Ratnakaram, Spectroscopic and laser properties of Er³⁺ doped fluoro-phosphate glasses as promising candidates for broadband optical fiber lasers and amplifiers, *Mater. Res. Bull.* 70 (2015) 935–944, <https://doi.org/10.1016/j.materresbull.2015.06.033>.
- [74] I. Konidakis, C.P.E. Varsamis, E.I. Kamitsos, D. Möncke, D. Ehrt, Structure and properties of mixed strontium–Manganese metaphosphate glasses, *J. Phys. Chem.* 114 (2010) 9125–9138, <https://doi.org/10.1021/jp101750t>.
- [75] M. Soltys, J. Pisarska, M. Leśniak, M. Sitarz, W.A. Pisarski, Structural and spectroscopic properties of lead phosphate glasses doubly doped with Tb³⁺ and Eu³⁺ ions, *J. Mol. Struct.* 1163 (2018) 418–427, <https://doi.org/10.1016/j.molstruc.2018.03.021>.
- [76] Q. Shi, Y. Yue, Y. Qu, S. Liu, G.A. Khater, L. Zhang, J. Zhao, J. Kang, Structure and chemical durability of calcium iron phosphate glasses doped with La₂O₃ and CeO₂, *J. Non-Cryst. Sol.* 516 (2019) 50–55, <https://doi.org/10.1016/j.jnoncrysol.2019.04.029>.
- [77] T.S. Gonçalves, R.J. Moreira Silva, M. de Oliveira Junior, C.R. Ferrari, G.Y. Poirier, H. Eckert, A.S.S. de Camargo, Structure–property relations in new fluorphosphate glasses singly- and co-doped with Er³⁺ and Yb³⁺, *Mater. Chem. Phys.* 157 (2015) 45–55, <https://doi.org/10.1016/j.matchemphys.2015.03.012>.
- [78] G. Liao, Q. Chem, J. Xing, H. Gebavi, D. Milanese, M. Fokine, M. Ferraris, Preparation and characterization of new fluorotellurite glasses for photonics application, *J. Non-Cryst. Sol.* 335 (2009) 447–452, <https://doi.org/10.1016/j.jnoncrysol.2009.01.011>.
- [79] D.L. Sidebottom, M. Hruschka, G.B. Potter, R.K. Brow, Increased radiative lifetime of rare earth-doped zinc oxyhalide tellurite glasses, *Appl. Phys. Lett.* 71 (1997) 1963–1965, <https://doi.org/10.1063/1.119756>.
- [80] A. Kaur, A. Khanna, L.I. Aleksandrov, Structural, thermal, optical and photoluminescent properties of barium tellurite glasses doped with rare-earth ions, *J. Non-Cryst. Sol.* 476 (2017) 67–74, <https://doi.org/10.1016/j.jnoncrysol.2017.09.025>.
- [81] J. Ozdanowa, H. Ticha, L. Tichy, Remark on the optical gap in ZnO–Bi₂O₃–TeO₂ glasses, *J. Non-Cryst. Sol.* 353 (2007) 2799–2802, <https://doi.org/10.1016/j.jnoncrysol.2007.06.017>.
- [82] W. Jastrzębski, M. Sitarz, M. Rokita, K. Butat, Infrared spectroscopy of different phosphates structures, *Spectrochim. Acta Mol. Biomol. Spectrosc.* 79 (2011)

- 722–727, <https://doi.org/10.1016/j.saa.2010.08.044>.
- [83] L. F Santos, R.M. Almeida, V.K. Tikhomirov, A. Jha, Raman spectra and structure of fluoroaluminophosphate glasses, *J. Non-Cryst. Sol.* 284 (2001) 43–48, [https://doi.org/10.1016/S0022-3093\(01\)00377-5](https://doi.org/10.1016/S0022-3093(01)00377-5).
- [84] G. Hou, C. Zhang, W. Fu, G. Li, J. Xia, Y. Ping, Broadband mid-infrared 2.0 μm and 4.1 μm emission in $\text{Ho}^{3+}/\text{Yb}^{3+}$ co-doped tellurite-germanate glasses, *J. Lumin.* 217 (2020) 116769, <https://doi.org/10.1016/j.jlumin.2019.116769>.
- [85] D. Ehrt, Structure and properties of fluoride phosphate glasses, *Proc. SPIE* 1761 (1993), <https://doi.org/10.1117/12.138929>.
- [86] D. Larink, M.T. Rinke, H. Eckert, Mixed network former effects in tellurite glass systems: structure/property correlations in the system $(\text{Na}_2\text{O})_{1/3}[(2\text{TeO}_2)_x(\text{P}_2\text{O}_5)_{1-x}]_{2/3}$, *J. Phys. Chem. C* 119 (31) (2015) 17539–17551, <https://doi.org/10.1021/acs.jpcc.5b04074>.
- [87] M.T. Rinke, L. Zhang, H. Eckert, Structural integration of tellurium oxide into mixed-network-former glasses: connectivity distribution in the system $\text{NaPO}_3\text{-TeO}_2$, *ChemPhysChem* 8 (2007) 1988–1998, <https://doi.org/10.1002/cphc.200700358>.